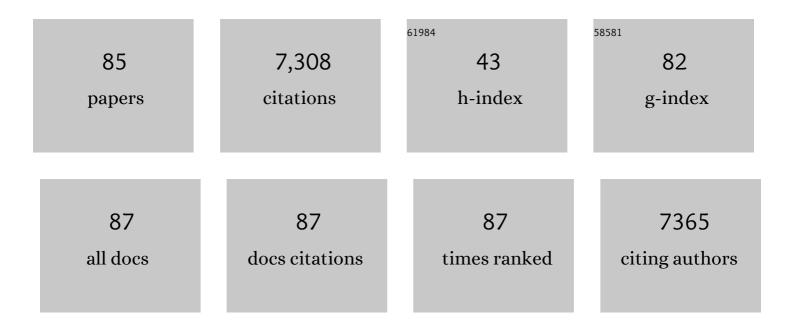
List of Publications by Year in descending order

Source: https://exaly.com/author-pdf/6253162/publications.pdf Version: 2024-02-01



#	Article	IF	CITATIONS
1	Boosting oxygen-reduction catalysis over mononuclear CuN2+2 moiety for rechargeable Zn-air battery. Chemical Engineering Journal, 2022, 430, 133105.	12.7	12
2	Electrodeposition of the manganese-doped nickel-phosphorus catalyst with enhanced hydrogen evolution reaction activity and durability. International Journal of Hydrogen Energy, 2022, 47, 41994-42000.	7.1	4
3	Electron accumulation enables Bi efficient CO2 reduction for formate production to boost clean Zn-CO2 batteries. Nano Energy, 2022, 92, 106780.	16.0	54
4	Trimetallic oxyhydroxides as active sites for large-current-density alkaline oxygen evolution and overall water splitting. Journal of Materials Science and Technology, 2022, 110, 128-135.	10.7	81
5	Preparation and characterization of Schiff base metal complexes for high performance supercapattery. Journal of Energy Storage, 2022, 48, 103956.	8.1	3
6	Sublayer-enhanced atomic sites of single atom catalysts through <i>in situ</i> atomization of metal oxide nanoparticles. Energy and Environmental Science, 2022, 15, 1183-1191.	30.8	25
7	Engineering Dual Singleâ€Atom Sites on 2D Ultrathin Nâ€doped Carbon Nanosheets Attaining Ultraâ€Lowâ€Temperature Zincâ€Air Battery. Angewandte Chemie - International Edition, 2022, 61, .	13.8	355
8	Bismuth with abundant defects for electrocatalytic CO ₂ reduction and Zn–CO ₂ batteries. Chemical Communications, 2022, 58, 3621-3624.	4.1	25
9	Low-temperature resistant gel polymer electrolytes for zinc–air batteries. Journal of Materials Chemistry A, 2022, 10, 19304-19319.	10.3	31
10	Quasi-solid-state Zn-air batteries with an atomically dispersed cobalt electrocatalyst and organohydrogel electrolyte. Nature Communications, 2022, 13, .	12.8	127
11	Boosting interfacial charge transfer for alkaline hydrogen evolution via rational interior Se modification. Nano Energy, 2021, 81, 105641.	16.0	118
12	Potential active sites of Mo single atoms for electrocatalytic reduction of N2. Chinese Chemical Letters, 2021, 32, 53-56.	9.0	66
13	Highly efficient oxygen evolution and stable water splitting by coupling NiFe LDH with metal phosphides. Science China Materials, 2021, 64, 1662-1670.	6.3	52
14	Phosphating-induced charge transfer on CoO/CoP interface for alkaline H2 evolution. Chinese Chemical Letters, 2021, 32, 3355-3358.	9.0	45
15	Defect-engineered 2D/2D hBN/g-C3N4 Z-scheme heterojunctions with full visible-light absorption: Efficient metal-free photocatalysts for hydrogen evolution. Applied Surface Science, 2021, 547, 149207.	6.1	51
16	Bimetallic chalcogenides for electrocatalytic CO2 reduction. Rare Metals, 2021, 40, 3442-3453.	7.1	47
17	One-stone, two birds: Alloying effect and surface defects induced by Pt on Cu2â ^{~,} xSe nanowires to boost C-C bond cleavage for electrocatalytic ethanol oxidation. Nano Energy, 2021, 88, 106307.	16.0	99
18	Deep oxidization of glucose driven by 4-acetamido-TEMPO for a glucose fuel cell at room temperature. Chemical Communications, 2021, 57, 4051-4054.	4.1	13

#	Article	IF	CITATIONS
19	Single Atom Catalysts for Fuel Cells and Rechargeable Batteries: Principles, Advances, and Opportunities. ACS Nano, 2021, 15, 210-239.	14.6	199
20	Engineering the Atomic Interface with Single Platinum Atoms for Enhanced Photocatalytic Hydrogen Production. Angewandte Chemie, 2020, 132, 1311-1317.	2.0	59
21	Engineering the Atomic Interface with Single Platinum Atoms for Enhanced Photocatalytic Hydrogen Production. Angewandte Chemie - International Edition, 2020, 59, 1295-1301.	13.8	344
22	Designing Atomic Active Centers for Hydrogen Evolution Electrocatalysts. Angewandte Chemie - International Edition, 2020, 59, 20794-20812.	13.8	257
23	Regulating the coordination structure of metal single atoms for efficient electrocatalytic CO ₂ reduction. Energy and Environmental Science, 2020, 13, 4609-4624.	30.8	188
24	Accelerating charge transfer to enhance H ₂ evolution of defect-rich CoFe ₂ O ₄ by constructing a Schottky junction. Chemical Communications, 2020, 56, 14019-14022.	4.1	34
25	Rational designed Co@N-doped carbon catalyst for high-efficient H2S selective oxidation by regulating electronic structures. Chemical Engineering Journal, 2020, 401, 126038.	12.7	43
26	TpyCo ²⁺ â€Based Coordination Polymers by Waterâ€Induced Gelling Trigged Efficient Oxygen Evolution Reaction. Advanced Functional Materials, 2020, 30, 2000593.	14.9	31
27	Electrospun Inorganic Nanofibers for Oxygen Electrocatalysis: Design, Fabrication, and Progress. Advanced Energy Materials, 2020, 10, 1902115.	19.5	111
28	Biomass <i>in situ</i> conversion to Fe single atomic sites coupled with Fe ₂ O ₃ clusters embedded in porous carbons for the oxygen reduction reaction. Journal of Materials Chemistry A, 2020, 8, 20629-20636.	10.3	54
29	Engineering of Electronic States on Co ₃ O ₄ Ultrathin Nanosheets by Cation Substitution and Anion Vacancies for Oxygen Evolution Reaction. Small, 2020, 16, e2001571.	10.0	98
30	Atomic-scale engineering of chemical-vapor-deposition-grown 2D transition metal dichalcogenides for electrocatalysis. Energy and Environmental Science, 2020, 13, 1593-1616.	30.8	166
31	Design aktiver atomarer Zentren für HERâ€Elektrokatalysatoren. Angewandte Chemie, 2020, 132, 20978-20998.	2.0	18
32	NiCoP nanoleaves array for electrocatalytic alkaline H2 evolution and overall water splitting. Journal of Energy Chemistry, 2020, 50, 395-401.	12.9	103
33	Biomass Waste-Derived 3D Metal-Free Porous Carbon as a Bifunctional Electrocatalyst for Rechargeable Zinc–Air Batteries. ACS Sustainable Chemistry and Engineering, 2019, 7, 17039-17046.	6.7	74
34	Enhanced Selective H ₂ S Oxidation Performance on Mo ₂ C-Modified g-C ₃ N ₄ . ACS Sustainable Chemistry and Engineering, 2019, 7, 16257-16263.	6.7	39
35	The functionality of surface hydroxyls on selective CH ₄ generation from photoreduction of CO ₂ over SiC nanosheets. Chemical Communications, 2019, 55, 1572-1575.	4.1	19
36	Charge Engineering of Mo2C@Defect-Rich N-Doped Carbon Nanosheets for Efficient Electrocatalytic H2 Evolution. Nano-Micro Letters, 2019, 11, 45.	27.0	86

#	Article	IF	CITATIONS
37	Confining ultrasmall bimetallic alloys in porous N–carbon for use as scalable and sustainable electrocatalysts for rechargeable Zn–air batteries. Journal of Materials Chemistry A, 2019, 7, 12451-12456.	10.3	128
38	Metal Organic Framework-Templated Synthesis of Bimetallic Selenides with Rich Phase Boundaries for Sodium-Ion Storage and Oxygen Evolution Reaction. ACS Nano, 2019, 13, 5635-5645.	14.6	400
39	Defect engineering in earth-abundant electrocatalysts for CO ₂ and N ₂ reduction. Energy and Environmental Science, 2019, 12, 1730-1750.	30.8	439
40	Ultrathin SiC Nanosheets with High Reduction Potential for Improved CH ₄ Generation from Photocatalytic Reduction of CO ₂ . ChemistrySelect, 2019, 4, 2211-2217.	1.5	15
41	Carbon nanotube-encapsulated cobalt for oxygen reduction: integration of space confinement and N-doping. Chemical Communications, 2019, 55, 14801-14804.	4.1	85
42	N-doped defective carbon with trace Co for efficient rechargeable liquid electrolyte-/all-solid-state Zn-air batteries. Science Bulletin, 2018, 63, 548-555.	9.0	117
43	Pyridinic-N-Dominated Doped Defective Graphene as a Superior Oxygen Electrocatalyst for Ultrahigh-Energy-Density Zn–Air Batteries. ACS Energy Letters, 2018, 3, 1183-1191.	17.4	456
44	Fe/Fe ₃ C@C nanoparticles encapsulated in N-doped graphene–CNTs framework as an efficient bifunctional oxygen electrocatalyst for robust rechargeable Zn–air batteries. Journal of Materials Chemistry A, 2018, 6, 516-526.	10.3	366
45	In Situâ€Fabricated 2D/2D Heterojunctions of Ultrathin SiC/Reduced Graphene Oxide Nanosheets for Efficient CO ₂ Photoreduction with High CH ₄ Selectivity. ChemSusChem, 2018, 11, 4237-4245.	6.8	48
46	Combined Electron and Structure Manipulation on Fe-Containing N-Doped Carbon Nanotubes To Boost Bifunctional Oxygen Electrocatalysis. ACS Applied Materials & Interfaces, 2018, 10, 35888-35895.	8.0	77
47	Potassium vanadates with stable structure and fast ion diffusion channel as cathode for rechargeable aqueous zinc-ion batteries. Nano Energy, 2018, 51, 579-587.	16.0	425
48	Growth of TiO2 nanostructures exposed {001} and {110} facets on SiC ultrafine fibers for enhanced gas sensing performance. Sensors and Actuators B: Chemical, 2018, 276, 57-64.	7.8	32
49	Edge Defect Engineering of Nitrogen-Doped Carbon for Oxygen Electrocatalysts in Zn–Air Batteries. ACS Applied Materials & Interfaces, 2018, 10, 29448-29456.	8.0	110
50	Facile synthesis of FeCo@NC core–shell nanospheres supported on graphene as an efficient bifunctional oxygen electrocatalyst. Nano Research, 2017, 10, 2332-2343.	10.4	85
51	Black Phosphorus/TiO ₂ Composite Photoanode with Enhanced Photoelectrical Performance. ChemElectroChem, 2017, 4, 2373-2377.	3.4	24
52	Nâ€Doped 3D Carbon Aerogel with Trace Fe as an Efficient Catalyst for the Oxygen Reduction Reaction. ChemElectroChem, 2017, 4, 514-520.	3.4	43
53	Oxygen-rich carbon-nitrogen quantum dots as cocatalysts for enhanced photocatalytic H 2 production activity of TiO 2 nanofibers. Progress in Natural Science: Materials International, 2017, 27, 333-337.	4.4	17
54	Astridia velutina-like S, N-codoped hierarchical porous carbon from silk cocoon for superior oxygen reduction reaction. RSC Advances, 2016, 6, 73560-73565.	3.6	15

#	Article	IF	CITATIONS
55	N-doped graphene grown on silk cocoon-derived interconnected carbon fibers for oxygen reduction reaction and photocatalytic hydrogen production. Nano Research, 2016, 9, 2498-2509.	10.4	70
56	Mesoporous silicon carbide nanofibers with in situ embedded carbon for co-catalyst free photocatalytic hydrogen production. Nano Research, 2016, 9, 886-898.	10.4	85
57	Three-dimensional (3D) interconnected networks fabricated via in-situ growth of N-doped graphene/carbon nanotubes on Co-containing carbon nanofibers for enhanced oxygen reduction. Nano Research, 2016, 9, 317-328.	10.4	70
58	Vertical SnO ₂ nanosheet@SiC nanofibers with hierarchical architecture for high-performance gas sensors. Journal of Materials Chemistry C, 2016, 4, 295-304.	5.5	75
59	Modification of hierarchically porous SiC ultrafine fibers with tunable nitrogen-containing surface. Ceramics International, 2016, 42, 5368-5374.	4.8	13
60	Tailoring of Porous Structure in Macro-Meso-Microporous SiC Ultrathin Fibers <i>via</i> Electrospinning Combined with Polymer-Derived Ceramics Route. Materials and Manufacturing Processes, 2016, 31, 1357-1365.	4.7	16
61	Electrospun interconnected Fe-N/C nanofiber networks as efficient electrocatalysts for oxygen reduction reaction in acidic media. Scientific Reports, 2015, 5, 17396.	3.3	65
62	A simply prepared flexible SiBOC ultrafine fiber mat with enhanced high-temperature stability and chemical resistance. RSC Advances, 2015, 5, 64911-64917.	3.6	20
63	Ultra-thin Cu ₂ S nanosheets: effective cocatalysts for photocatalytic hydrogen production. Chemical Communications, 2015, 51, 13305-13308.	4.1	35
64	Scalable in situ growth of SnO2 nanoparticle chains on SiC ultrathin fibers via a facile sol–gel-flame method. Applied Surface Science, 2015, 335, 208-212.	6.1	19
65	B, N-codoped 3D micro-/mesoporous carbon nanofibers web as efficient metal-free catalysts for oxygen reduction. Current Applied Physics, 2015, 15, 1606-1614.	2.4	34
66	In situ synthesis of graphitic-C3N4 nanosheet hybridized N-doped TiO2 nanofibers for efficient photocatalytic H2 production and degradation. Nano Research, 2015, 8, 1199-1209.	10.4	292
67	Flexible N–doped TiO2/C ultrafine fiber mat and its photocatalytic activity under simulated sunlight. Applied Surface Science, 2014, 319, 136-142.	6.1	30
68	Hierarchically porous SiC ultrathin fibers mat with enhanced mass transport, amphipathic property and high-temperature erosion resistance. Journal of Materials Chemistry A, 2014, 2, 20873-20881.	10.3	86
69	Large-scale, flexible and high-temperature resistant ZrO ₂ /SiC ultrafine fibers with a radial gradient composition. Journal of Materials Chemistry A, 2014, 2, 9607-9612.	10.3	49
70	Preparation and photocatalytic activity of N–Ag co-doped TiO2/C porous ultrafine fibers mat. Ceramics International, 2014, 40, 2017-2022.	4.8	10
71	Enhanced photocatalytic CO2-reduction activity of electrospun mesoporous TiO2 nanofibers by solvothermal treatment. Dalton Transactions, 2014, 43, 9158.	3.3	105
72	Atmosphere influence in the pyrolysis of poly[(alkylamino)borazine] for the production of BN fibers. Ceramics International, 2013, 39, 6847-6851.	4.8	21

#	Article	IF	CITATIONS
73	Influence of pyrolysis conditions on fabrication of polymer-derived BN fiber for wave transparent application. Composites Part B: Engineering, 2013, 51, 254-259.	12.0	24
74	Effect of Temperature on the Composition and Properties of Poly[(alkylamino)borazine] Precursor to Boron Nitride. Journal of Macromolecular Science - Physics, 2013, 52, 1427-1437.	1.0	5
75	A Novel Liquid Poly[(Alkylamino)Borazine] for Boron Nitride. Materials and Manufacturing Processes, 2012, 28, 14-18.	4.7	0
76	Boron nitride by pyrolysis of the melt-processable poly[tris(methylamino)borane]: Structure, composition and oxidation resistance. Ceramics International, 2012, 38, 271-276.	4.8	37
77	Pyrolysis behavior of poly[(n-propylamino/methylamino)borazine]. Ceramics International, 2012, 38, 4745-4749.	4.8	7
78	Ammonia curing behavior of poly[(alkylamino)borazine] fiber. Materials Letters, 2012, 71, 91-93.	2.6	7
79	Influence of Monomer Structures on the High Temperature Properties of	0.2	1
80	Nearly stoichiometric BN fiber with low dielectric constant derived from poly[(alkylamino)borazine]. Materials Letters, 2011, 65, 157-159.	2.6	34
81	Effect of molecular monomer structure on the composition and properties of BN via the preceramic polymer route. Materials Letters, 2011, 65, 1111-1113.	2.6	10
82	Novel processable precursor for BN by the polymer-derived ceramics route. Ceramics International, 2011, 37, 3005-3009.	4.8	28
83	Nearly stoichiometric BN fiber by curing and thermolysis of a novel poly[(alkylamino)borazine]. Ceramics International, 2011, 37, 1795-1800.	4.8	18
84	Engineering Dual Singleâ€Atom Sites on 2D Ultrathin Nâ€doped Carbon Nanosheets Attaining Ultraâ€Lowâ€Temperature Zincâ€Air Battery. Angewandte Chemie, 0, , .	2.0	24
85	Multi-TpyCo ²⁺ -based conductive supramolecular hydrogels constructed by "bridge bond― for ultrastable rechargeable Zn-air battery over 1100 h. Journal of Materials Chemistry A, 0, , .	10.3	3